Binding and intracellular trafficking of lipoprotein lipase and triacylglycerol-rich lipoproteins by liver cells

Ricardo P. Casaroli-Marano,[1,*] Raquel García,[1,*] Elisabet Vilella,[†] Gunilla Olivecrona,[§] Manuel Reina,[*] and Senén Vilaró,[2,*]

Department of Cellular Biology,* Faculty of Biology, University of Barcelona, Avda. Diagonal, 645, E-08028 Barcelona, Spain; Centre de Recerca Biomèdica,[†] Hospital de Sant Joan, E-43201 Reus, Spain; and Department of Medical Biochemistry and Biophysics,[§] University of Umeå, S-901 87 Umeå, Sweden

Abstract The cellular mechanisms and pathways by which lipoprotein lipase (LPL) enhances the binding and uptake of lipoproteins remains unknown. Confocal and immunoelectron microscopy demonstrated that primary binding of bovine LPL (bLPL) occurs at the microvilli surface of HepG2 cells and hepatocytes. Internalized bLPL was associated with endocytic vesicles and multivesicular bodies. Quantitative immunofluorescence indicated that the presence of bLPL caused a marked increase in the cell-surface binding of *DiI*-conjugated triacylglycerol-rich lipoproteins (*DiI*-TRL). Confocal microscopy showed that when *DiI*-TRL was incubated with bLPL at 4°C, the distributions of bound LPL and *DiI*-TRL were totally coincident, and covered the apical surface of both HepG2 cells and hepatocytes. When incubated separately, the time-courses of the internalization of fluorescence associated with *DiI*-TRL and bLPL were different: *DiI*-TRL was quickly internalized by both HepG2 cells and hepatocytes, and reached a plateau at 30 min, whereas intracellular LPL increased continuously, but more slowly in the same period. In the presence of bLPL, *DiI*-TRL was internalized progressively by HepG2 and by cultured hepatocytes for up to 1 h and no saturation was reached. At this time the intensity of labeling of bLPL was lower than of *DiI*-TRL and a higher number of *DiI* spots did not colocalize with bLPL immunofluorescence, suggesting that the ligands follow a different pathway after internalization. The data suggest that when lipoprotein lipase (LPL) is associated with the lipoproteins it directs them to specific endocytic pathways. A hypothetical model of the intracellular pathways followed by triacylglycerol-rich lipoproteins and LPL after internalization is proposed.—**Casaroli-Marano, R. P., R. García, E. Vilella, G. Olivecrona, M. Reina, and S. Vilaró.** Binding and intracellular trafficking of lipoprotein lipase and triacylglycerol-rich lipoproteins by liver cells. *J. Lipid Res.* 1998. **39:** 789–806.

Supplementary key words immunofluorescence • immunoelectron microscopy • lipoprotein • heparan sulfate proteoglycans • confocal microscopy

Fatty acids are delivered to the peripheral tissues by two types of triacylglycerol-rich lipoproteins (TRL): chylomicrons, which are synthesized in the intestine and transport dietary lipids to various tissues, and very low density lipoproteins (VLDL), which are synthesized in the liver and transport endogenous lipids. In the circulation they undergo diverse modifications such as acquisition of apolipoproteins from other circulating lipoproteins and hydrolysis of their triacylglycerides, catalyzed by lipoprotein lipase (LPL; EC 3.1.1.34) (see 1, 2 for recent reviews). The resulting lipoproteins, known as remnant particles, are smaller and denser, and have altered lipid and apolipoprotein composition. These new particles are quickly catabolized by the liver. Apolipoprotein (apo) conformational changes and composition on the particle surface, such as the enrichment of apoE, on the particle surface are determinants for the recognition of hepatic receptors (3). Several studies indicate that the uptake of chylomicron remnants by hepatocytes is mediated by apoE, which serves as the ligand for liver-specific receptors present in the space of Disse (3).

Felts, Itakura, and Crane (4) proposed that lipoprotein lipase (LPL) could be a recognition signal for remnant uptake by the liver. Although LPL is synthesized in extrahepatic tissues it circulates in blood associated with lipoproteins (5, 6) and is cleared by the liver (7, 8). Since the pioneering work of Beisiegel, Weber, and Bengtsson-Olivecrona (9) and Mulder, de Wit, and Havekes (10), several studies have shown that LPL enhances the binding and uptake of lipoproteins by cultured hepatoma cells and hepatocytes (11–24). LPL also potentiates the uptake of lipoproteins and lipid emulsions in perfused rat livers (8, 25). Both LPL activ-

Abbreviations: LPL, lipoprotein lipase; bLPL, bovine LPL; LDL, low density lipoprotein; LDLr, LDL receptor; LRP, LDL receptor-related protein; HSPG, heparan sulfate proteoglycans; TRL, triacylglcerol-rich lipoprotein; VLDL, very low density lipoproteins; VLDLr, VLDL receptor.

[1] The first two authors contributed equally to this paper.

[2] To whom correspondence should be addressed.

ity and LPL structure seem to be involved in this mediated uptake (reviewed by 1, 26, 27). Activity is important for the remodeling of TRL into remnant particles and structure for the bridge action of LPL between the lipoprotein particle and the cell surface (28). Inactive LPL also potentiates efficient binding and catabolism of TRL (25). However, the cellular mechanisms of LPL binding and uptake seem to be rather complex and the function and physiological relevance are not fully understood.

LPL could bind to at least three plasma membrane receptors. *i*) Heparan sulfate proteoglycans (HSPG) are the most abundant and widely expressed LPL-binding molecules (26) present at the surface of most cells. The glycosaminoglycans heparan sulfate and heparin bind LPL with high association and dissociation rate constants, which suggests that the enzyme moves rapidly between binding sites (29). Several studies have shown that HSPG are critical both for LPL binding and for LPL-mediated binding of lipoproteins to the plasma membrane of HepG2 cells (11–14, 16–19, 21, 23, 24). *ii*) The α_2-macroglobulin receptor/low density lipoprotein receptor-related protein (hereafter referred to as LRP) bind LPL as demonstrated by cross-linking experiments in cultured cells (9) and by solid-phase assays (30–33). LPL mediates binding of lipoproteins to LRP and promotes its intracellular catabolism (30, 34). *iii*) Several recent reports have shown that other members of the LDL receptor gene family, such as the LDL receptor itself (35), the VLDL receptor (VLDLr) (36, 37), and the GP330/LRP2 (38, 39) could bind LPL and influence LPL-mediated lipoprotein catabolism. To integrate all these receptors a model has been postulated in which the initial LPL-binding sites could be the plasma membrane HSPG, whereby the interaction of lipoproteins with other plasma membrane receptors (such LRP or LDLr) for uptake and catabolism of the extracellular ligands (1, 26, 27 for reviews) could be facilitated.

Recent studies in our laboratory (40–42) demonstrated that human fibroblasts organize bLPL-binding sites in parallel linear arrays that cross the fibroblast cell surface longitudinally. To assess the intracellular transport of LPL and LPL-lipoprotein complexes in HepG2 cells and in hepatocytes, we performed quantitative studies by fluorescence and immunogold techniques. The results provide evidence that the mechanisms for binding and uptake of TRL could be different in the presence and absence of LPL.

MATERIALS AND METHODS

Chemicals and antibodies

Dubelcco's modified eagle's medium (DMEM) with 1 g/l glucose, E-199 medium and fetal calf serum were obtained from Bio-Whittaker (Boehringer Ingelheim, Verviers, Belgium). Bovine serum albumin (BSA; fraction V, essentially fatty acid-free), ovalbumin, gelatin, glycine, heparin, glutamine, penicillin, streptomycin, sucrose, dimethyl sulfoxide, ammonium chloride, and Triton X-100 were from Sigma Chemicals (St. Louis, MO). Mowiol mounting medium was from Calbiochem (La Jolla, CA). *DiI* (1,1′-dictadecyl-3,3,3′,3′-tetramethylindocarbocyanine perchlorate) was purchased from Molecular Probes (Leiden, The Netherlands). HEPES and collagenase A were obtained from Boehringer-Mannheim (Mannheim, Germany). Bovine LPL (bLPL) was purified from milk as previously described (43). The secondary antibody *FITC* (fluorescein isothiocyanate)-conjugated rabbit anti-mouse was from Dakoppats (Grostrup, Denmark) and secondary rabbit IgG against chicken was from Nordic (Tilburg, The Netherlands). Paraformaldehyde and glutaraldehyde fixatives and uranyl acetate were from Merck (Darmstadt, Germany). Protein A conjugated to gold 15 nm (pA-Au 15 nm) was purchased from Dr. Hans Slot (University of Utrecht, The Netherlands). All other reagents were of the highest purity available. Primary antibodies to bovine LPL were: the monoclonal 5D2 antibody against bLPL from Oncogene (Uniondale, NY) and the affinity-purified chicken antibody against bLPL (41).

Cell isolation and culture

Hepatocytes from adult rats were obtained by a modification of the method of Berry and Friend (44) using in situ perfusion of the liver with collagenase. Cell suspension was filtered through a double-layered nylon 100-mesh gauze and centrifuged twice for 3 min at 50 *g*. The resulting pellet was a mixture of hepatocytes and hematopoietic cells. To separate these cell types the pellet was suspended and centrifuged twice at 30 *g* for 1 min and then twice at 15 *g* for 1 min. The hepatocyte fraction was placed on 80-mm diameter tissue culture dishes (Corning, New York, NY), with glass coverslips, at a density of 100,000 cells/cm^2 in E-199 medium supplemented with 10% fetal calf serum, 2 mm glutamine, 100 U/ml penicillin, and 100 mg/ml streptomycin, at 37°C in a humidified 5% CO_2 and 95% air atmosphere. A 1% gelatin coat on the glass coverslips was added to facilitate the attachment of the hepatocytes. Experiments were performed 24 h after isolation.

HepG2 cells were grown in 80-mm or 35-mm diameter tissue culture dishes in DMEM, supplemented with 10% fetal calf serum, containing glutamine and antibiotics. For immunofluorescence experiments, the cells were plated on glass coverslips without gelatin and grown as indicated above.

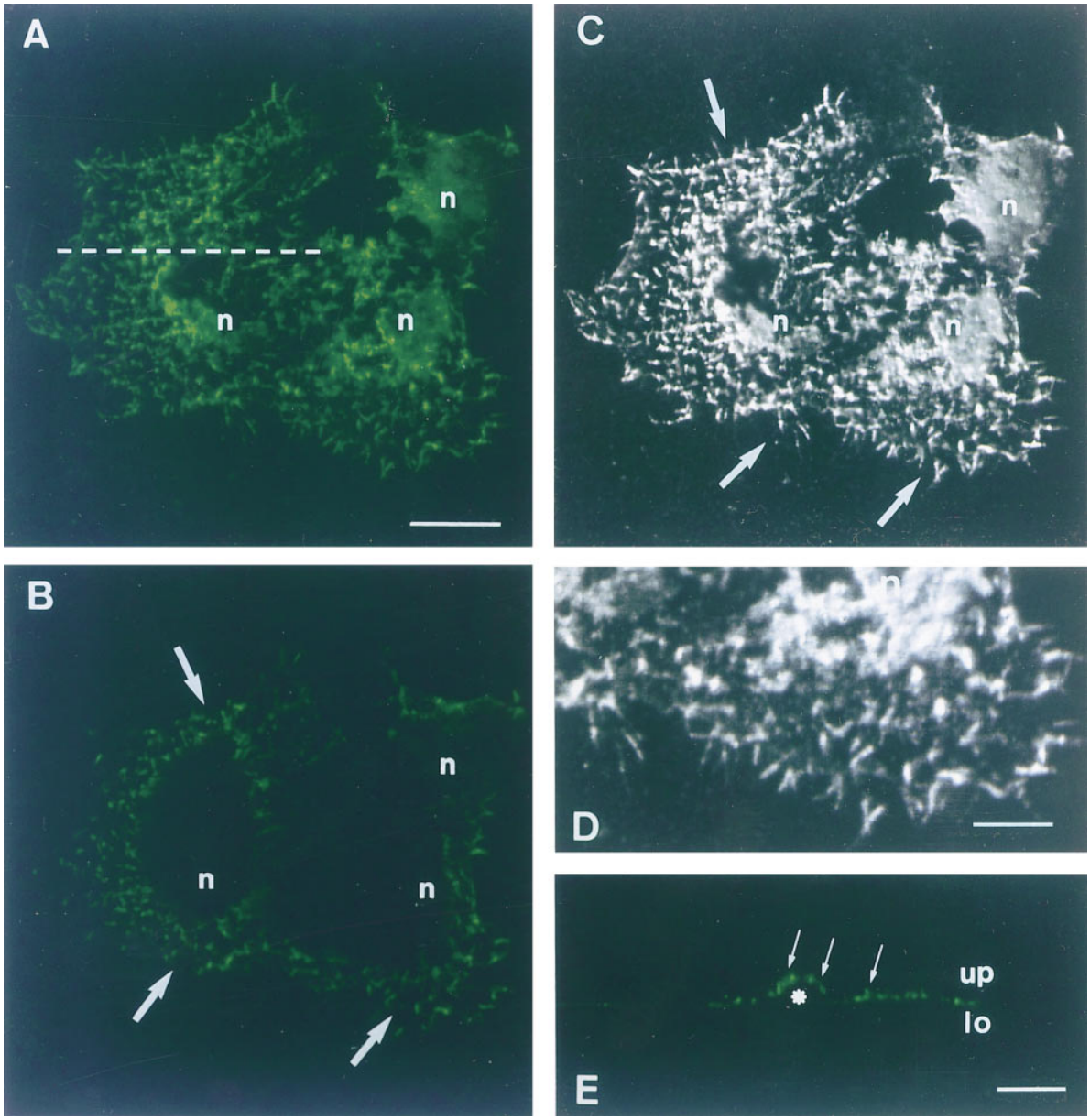

Fig. 1. Binding of bLPL on HepG2 cells by immunofluorescence on confocal microscopy. HepG2 cells were incubated with bLPL for 45 min at 4°C. The cells were fixed, and bLPL was then detected by monoclonal 5D2 antibody followed by *FITC*-conjugated rabbit anti-mouse immunoglobulins. (A) A three-dimensional projection of six horizontal sections (*xy*, 0.31 μm; step size 0.72 μm). (B) A single horizontal section of panel A, taken from the middle of the cells. (C) A Simulated Fluorescence Process image showing discrete structures that are labeled with the anti-LPL (arrows in B and C). (D) A high magnification of the bottom-right area of panel C. (E) A vertical section (*xz*; 0.90 μm), taken as indicated by the dotted line drawn in panel A, showing bLPL bound in the upper (up) part of the cell (arrows). Bar for A, B, C, and E: 10 μm. Bar for D: 5 μm. n and asterisk: nucleus; lo: lower part of the cell.

Human lipoprotein isolation and labeling

Blood was collected from fasted hypertriglyceridemic (type IV hyperlipidemia) subjects and plasma was pooled to isolate TRL ($d < 1.006$ g/ml) by preparative ultracentrifugation. All subjects included had an E3/E3 apoE genotype. Labeling of TRL was performed following the protocol described by Innerarity, Pitas, and Mahley (45). Briefly, 0.5 mg/ml of TRL was incubated with 100 μl of *DiI* dissovled in dimethyl sulfoxide (3 mg/ml) in the presence of lipoprotein-deficient human serum for 8 h at 37°C in the dark. Then, the mixture was overlaid with PBS (10 mm phosphate, 150 mm NaCl, pH 7.4) to isolate the *DiI*-TRL. Free dye was separated by ultracentrifugation (300,000 *g*, 16 h at 4°C).

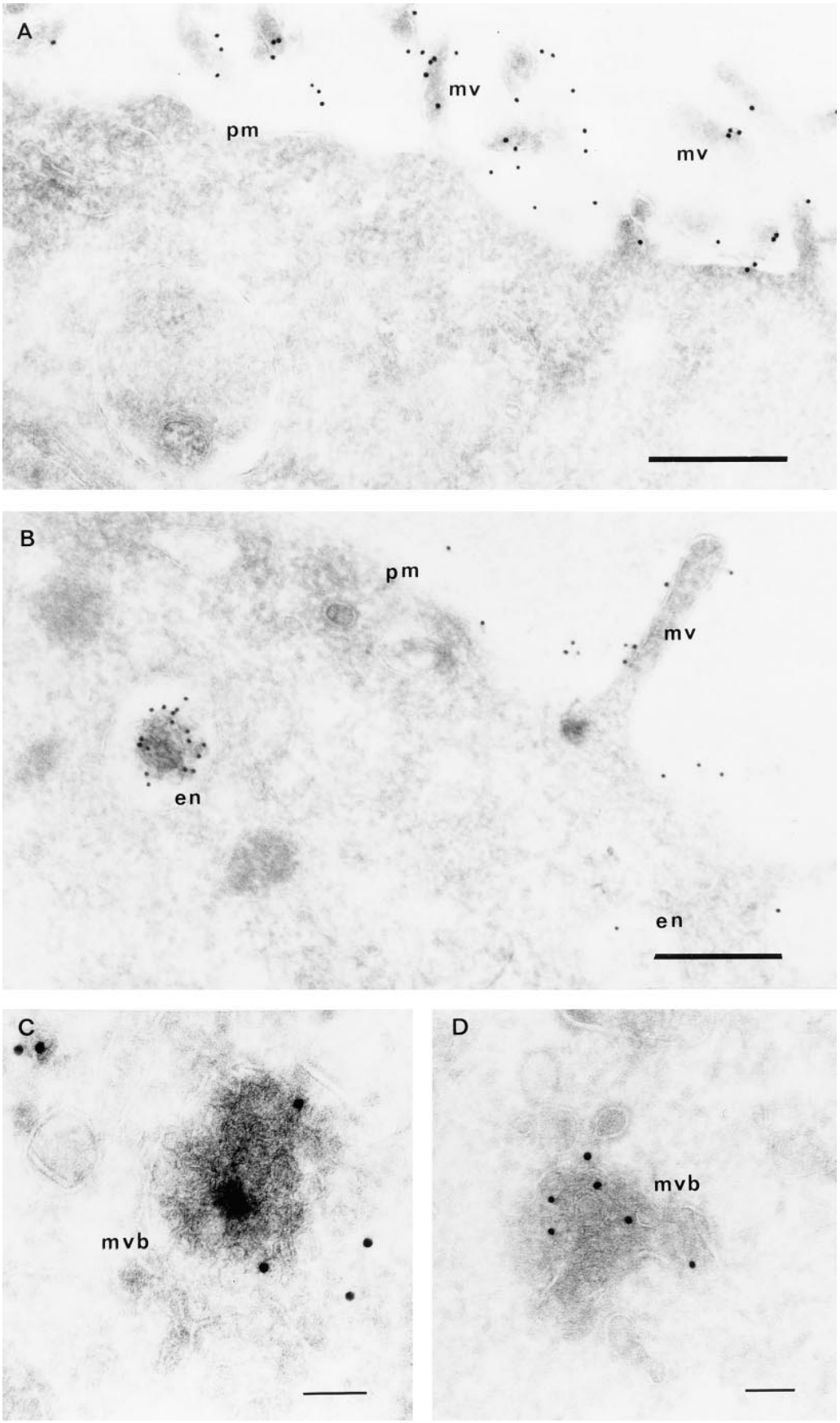

DiI-TRLs were then dialyzed against PBS and filtered before use. Protein content was determined by the BCA method (Pierce, Rockford, IL) using BSA as a standard. To assess the presence of apoB, samples were delipidated and the redissolved protein was subjected to electrophoresis in an 8–18% gradient polyacrylamide gel; then the protein bands were transferred to a nitrocellulose membrane. ApoB was visualized using a goat polyclonal antibody against apoB followed by an incubation with a rabbit Ig-POD-conjugated anti-goat. ECL was used as the developing system. The fluorogram showed a major band with a molecular mass of 550 kDa corresponding to apoB-100 and second band (about three times lower) with a molecular mass of 250 kDa corresponding to apoB-48. This result indicates that TRL from type IV patients, isolated as particles with a $d < 1.006$ g/L, contain both chylomicrons and VLDL. These particles with a triacylglyceride-to-cholesterol ratio of 2.7 and a protein content of 0.9 mg/ml were used as a model of remnant particles in cell binding and internalization assays.

Binding and internalization experiments

For the bindings experiments, cells (on coverslips or 35 mm dishes) were rinsed in DMEM at 4°C, prechilled for 30 min at 4°C in the same medium, and incubated for 45 min at 4°C with 2.5 μg/ml of bLPL in DMEM–20 mm HEPES, pH 7.4, containing 1% BSA. The cells were then washed in DMEM–20 mm HEPES, and finally processed for immunofluorescence or immunoelectron microscopy. *DiI*-TRL (≈10 μg/ml) was added to the cells either in the presence or in the absence of 2.5 μg/ml of bLPL following the protocol described above. In parallel experiments, heparin was added to the binding medium to a final concentration of 50 U/ml. Uptake of bLPL and TRL was assessed by incubating the cells for different periods (3, 15, 30, and 60 min) at 37°C after binding of bLPL and lipoproteins at 4°C for 45 min. After each period, cells were washed in DMEM–20 mm HEPES. Alternatively, to examine uptake of TRL, cells were washed in DMEM–20 mm HEPES containing heparin 50 U/ml. Cells were then fixed in 3% paraformaldehyde–2% sucrose in 100 mm phosphate buffer, pH 7.4, for 30 min at room temperature. For immunodetection of bLPL, cells were processed as described below.

Immunofluorescence experiments

Fixed cells were rinsed twice in PBS–20 mm glycine (10 mm phosphate, 150 mm NaCl, 20 mm glycine, pH 7.4). For the internalization experiments cells were permeabilized with PBS containing 0.1% Triton X-100 for 10 min and rinsed in PBS–20 mm glycine. Cells were then blocked with PBS–20 mm glycine containing 1% BSA, for 10 min at room temperature. For immunodetection of bound bLPL the primary 5D2 antibody, at 1:100 dilution, was incubated for 1 h at 37°C in a humid chamber. *FITC*-conjugated rabbit anti-mouse at 1:50 dilution was applied and incubated for 45 min at 37°C in darkness. Both antibodies were diluted in blocking solution. After successive washes in PBS, the coverslips were mounted upside-down on a glass slide with 5 μl of Mowiol. Control coverslips without primary antibody were processed in parallel. The cells were observed using a Zeiss Axioskop (Carl Zeiss, Oberkochen, Germany) epifluorescence illumination microscope and a Leica TCS 4D (Leica Lasertechnik GmbH, Heidelberg, Germany) confocal scanning laser microscope.

Confocal scanning laser microscopy

For the acquisition of digital images at two fluorescence emission wavelengths, the Leica TCS 4D confocal scanning laser microscope was adapted to an inverted Leitz DMIRBE microscope and a 63× (NA 1.4, oil) Leitz Plan-Apo objective. The light source was an argon–krypton laser 75 mW. *FITC* (bLPL) and *DiI* (TRL) were excited at 488 and 568 nm with the laser. Image sizes were 512 × 512 and three-dimensional projection images were calculated from six serial optical sections. Voxel dimensions were 0.31 μm lateral and 0.5 μm axial. For vertical sections $\{x,z\}$ the pixel size was 0.2 μm. In ther internalization figure, four serial sections with 0.96 μm vertical distance ($\{x,y\}$ pixel size, 0.31 μm) were taken. Final images were obtained by a color high resolution video printer (Mitsubishi CP2000E).

Fluorescence quantification

Fluorescence microscopy and digital image collection were performed using a Zeiss Axioskop epifluorescence microscope (63×, NA 1.4) equipped with a Hamamatsu Photonics chilled CCD camera (C5985 model, Hamamatsu Photonic K.K., Japan) on a COMPAQ prolinea station 4/50 computer system. Fluorescence

Fig. 2. Binding and internalization of bLPL by HepG2. After binding of bLPL, performed as in Fig. 1, cells were washed and incubated for 30 or 60 min at 37°C and fixed, and cryoultrasections were obtained. bLPL was detected by chicken anti-bLPL, followed a secondary rabbit anti-chicken IgG and protein A-colloidal gold (15 nm) as described in Materials and Methods. (A) After binding, bLPL was almost exclusively associated with microvilli (mv). (B) After 30 min at 37°C, some bLPL was detected in vesicular structures resembling endosomes (en). However, a large number of immunogold particles are still associated with microvilli. (C) and (D) After 60 min of incubation, intracellular bLPL was located in multivesicular bodies (mvb). pm: plasma membrane. Bar for A and B: 0.5 μm; Bar for C and D: 0.1 μm.

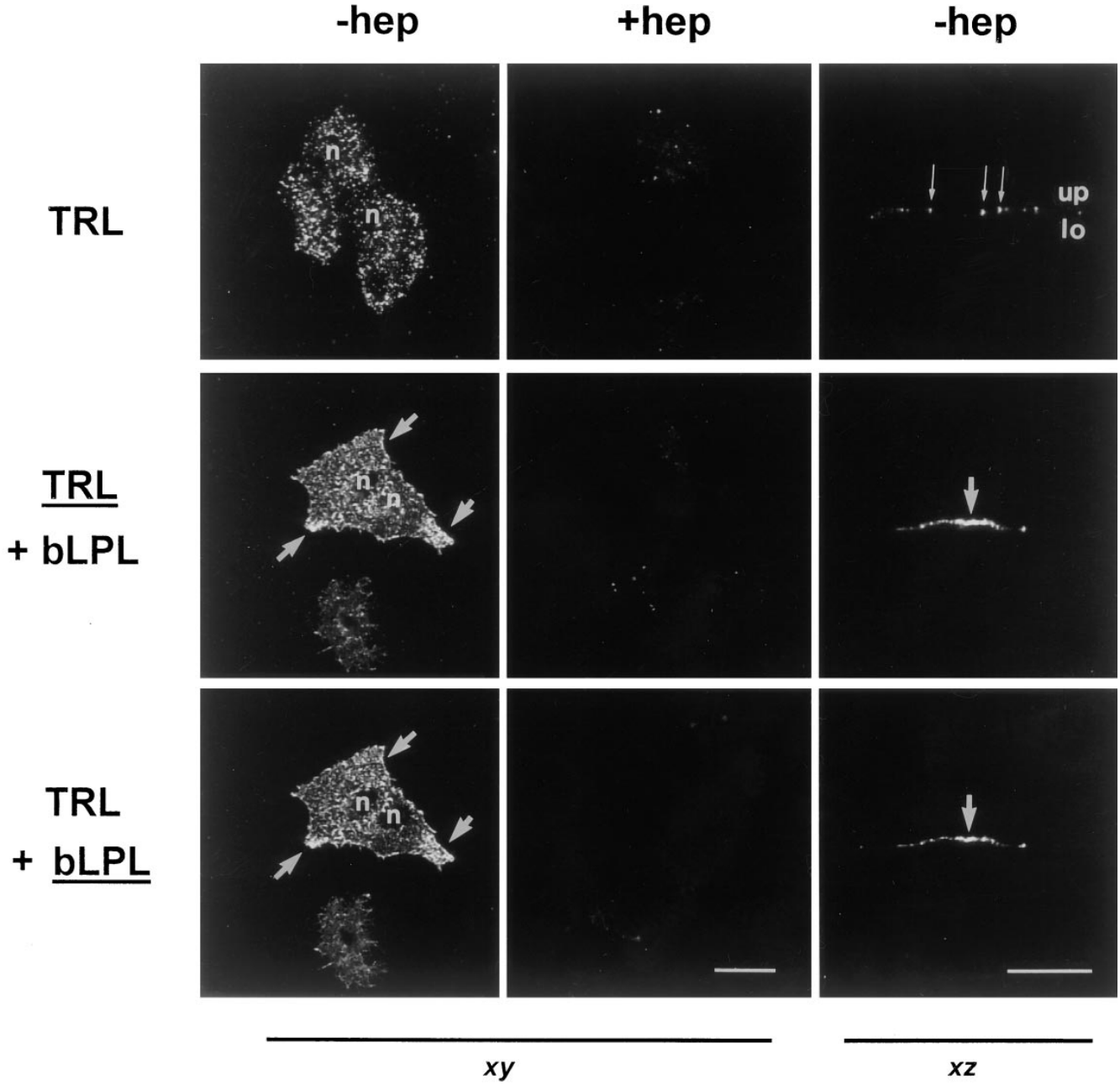

Fig. 3. Binding of *DiI*-TRL by HepG2 cells in the presence or absence of bLPL. HepG2 cells were incubated for 45 min at 4°C with *DiI*-TRL, with or without bLPL, and in the presence (+hep) or absence (−hep) or heparin (50 U/ml). After washing and fixation, bLPL was detected by monoclonal 5D2 antibody followed by *FITC*-conjugated rabbit anti-mouse immunoglobulins. A three-dimensional projection of six horizontal sections (*xy*, 0.31 μm; step size 0.73 μm) and vertical sections (*xz*, 0.85 μm) was viewed by a confocal microscope. Images correspond to the fluorescence of the ligand underlined. In the absence of bLPL, *DiI*-TRL (TRL) showed a discontinuous punctate fluorescence pattern as viewed in *xz* (fine arrows). In the *xy* projection, *DiI*-TRL in the presence of bLPL (TRL + bLPL) displayed an identical binding pattern (arrows) to those of bLPL (TRL + bLPL). Fluorescence covered all the upper (up) side of the cells, as visualized in an *xz* section (arrow). Heparin (+hep) abolished the cell surface-associated fluorescence for both *DiI*-TRL and bLPL. Bar for *xy* projections and for *xz* sections: 25 μm. n: nucleus; lo: lower side of the cells.

was quantified using the Argus-50 image analysis software (ver. 3.43, Hamamatsu Photonics, K.K.). Total fluorescence per field was obtained by summing the pixel intensity of an area defined by the shape of the cells. Fluorescence from eight different fields (at least 60,000 μm^2) was quantified for each experimental condition. Background fluorescence values including autofluorescence and non-specific fluorescence were obtained by

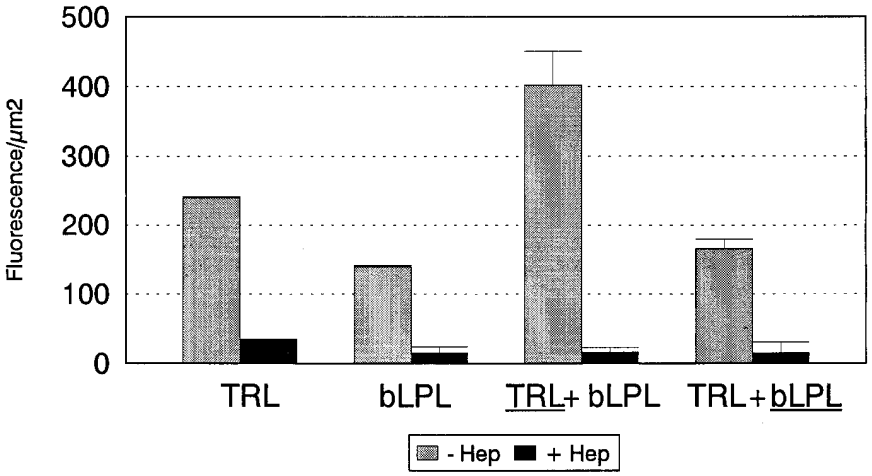

Fig. 4. Quantification of cell surface-associated fluorescence for *DiI*-TRL and bLPL. Experimental conditions were as indicated in Fig. 3. Heparin (+Hep) was used at 50 U/ml. Fluorescence quantification was performed by a CCD-video camera connected to a fluorescence image analysis system as described in Materials and Methods. Intensity of fluorescence per surface area (μm^2) is represented by mean ± SD from two consecutive and representative experiments. The area analyzed for each condition was of about 6,000 μm^2.

imaging fields of cells under the same illumination and exposure conditions (1s with gain 3).

Immunoelectron microscopy

Bovine LPL was added to HepG2 cells grown in 35-mm diameter culture dishes as described above. The cells were then washed twice in cold PBS and fresh medium was added. For studies of internalization the cells were incubated for different periods (0, 30, 60, and 120 min) at 37°C, washed in PBS, and finally fixed for 2 h with 2% paraformaldehyde–0.2% glutaraldehyde in 100 mm phosphate buffer (pH 7.4). After fixation, the cells were washed, scraped with a rubber policeman, and collected after centrifugation (1,000 *g*, 5 min). The cell pellet was embedded in 10% gelatin and postfixed with 2% paraformaldehyde in 100 mm phosphate buffer (pH 7.4) at 4°C overnight. Blocks were cryoprotected in polyvinylpyrrolidone and 2% sucrose solution for 24 h, mounted on a metal stub, rapidly frozen in liquid nitrogen, and stored at −196°C before microtomy. Ultracryothin sections (60 nm–85 nm) were obtained by ultracryomicrotomy with an FC4 system (Reichert Jung, Wien, Austria) at −105°C. Sections were collected on gold grids (200 mesh) formvar-coated for transmission electron microscopy, and maintained in 100 mm PBS, pH 7.4, at 4°C. The grids were treated with 150 mm ammonium chloride in 10 mm PBS solution, rinsed in 10 mm PBS–20 mm glycine solution, and then blocked in 1% ovalbumin in 10 mm PBS–20 mm glycine solution at room temperature. Grids were incubated with the affinity-purified chicken antibodies against bLPL, at 1:200 dilution, for 30 min at room temperature in a blocking solution. After several washes the sections were incubated for 30 min with a secondary rabbit IgG against chicken, at 1:1000 dilution. Finally, pA-Au 15 nm was added for 20 min and sections were then contrasted with 0.03% uranyl acetate solution and a thin surface membrane of methyl-cellulose was applied. Control experiments were performed in parallel by omitting either the bLPL or the primary antibody or both. Electron micrographs were obtained on a Hitachi 600 AB (Hitachi Corp., Tokyo, Japan). The intra- and extracellular distribution of LPL was determined by counting the number of gold particles located either at the plasma membrane or in intracellular vesicles, as previously described (41).

RESULTS

Binding and internalization of bLPL by HepG2 cells

HepG2 cells were incubated with bLPL at 4°C for 30 min and immunofluorescence was analyzed by confocal microscopy (**Fig. 1**). The bLPL-binding appeared on discrete structures that resembled microvilli (Figs. 1B and C, arrows). The Simulated Fluorescence Projection (Figs. 1C and D), which displays the fluorescence in an object volume be a shading effect, suggested that bLPL bound mainly to the microvilli structures (Fig. 1D). Vertical sections performed with the confocal microscope indicate that bLPL-binding sites were located on the upper plasma membrane of HepG2 cells (Fig. 1E).

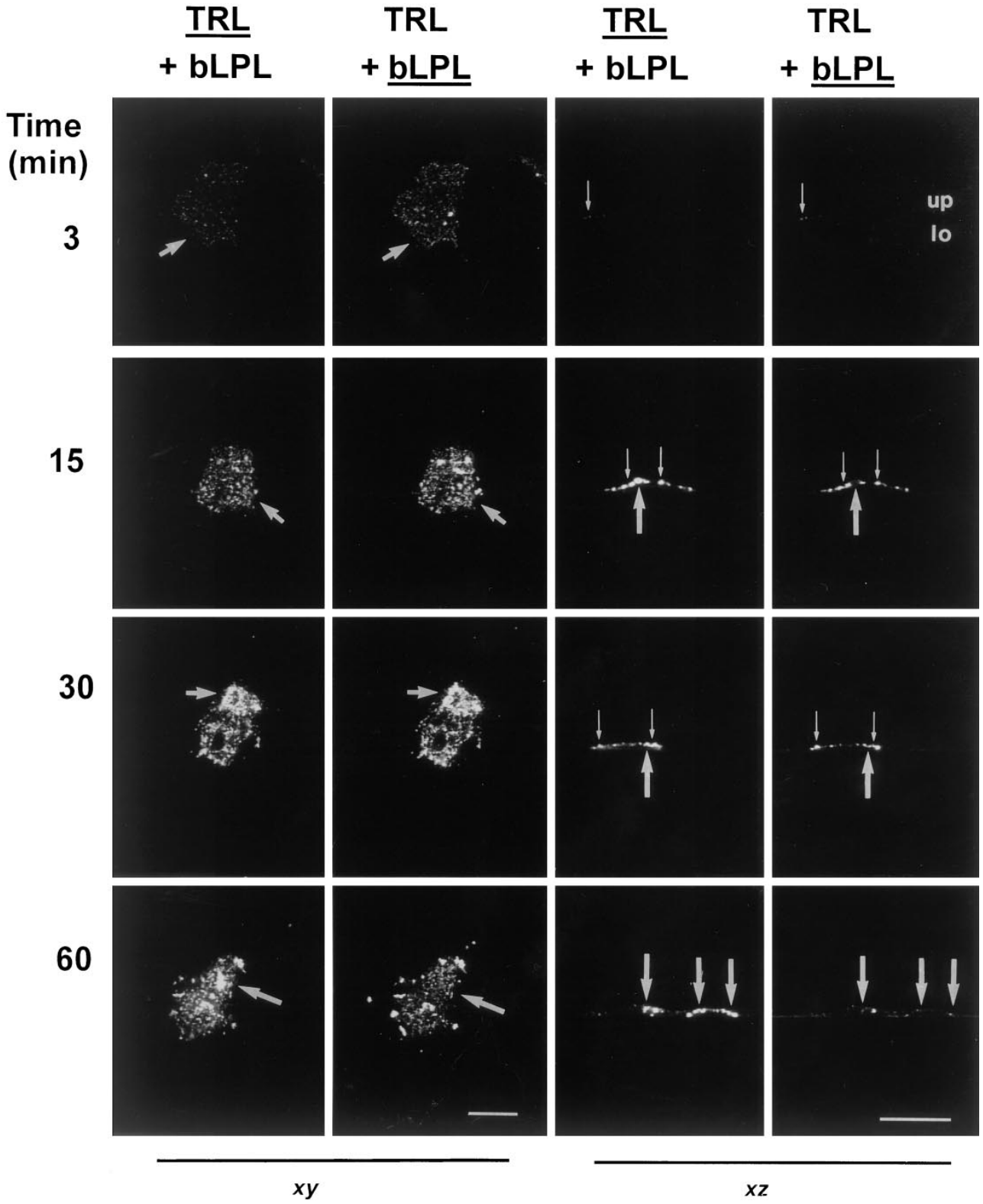

Figure 5.

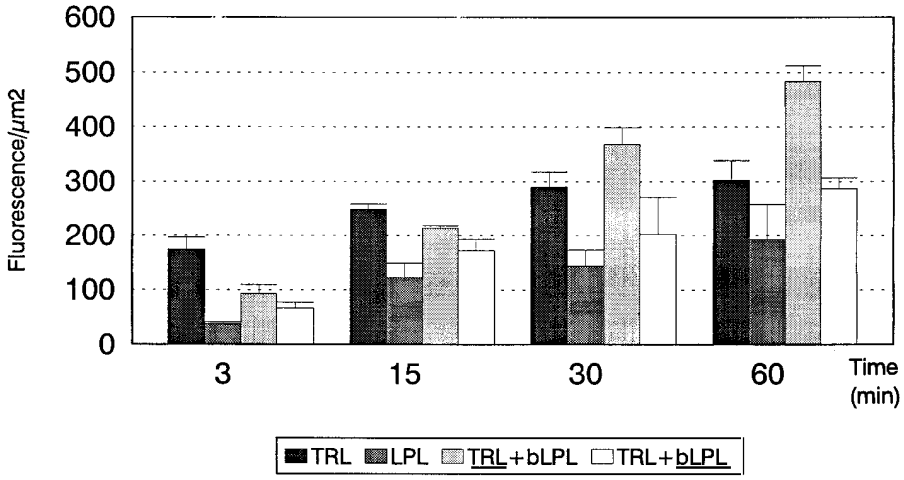

Fig. 6. Quantification of intracellular fluorescence of bLPL and *DiI*-TRL in the presence or absence of bLPL. HepG2 cells were incubated for 45 min at 4°C with bLPL and *DiI*-TRL in the presence or absence of bLPL, and incubated for 3, 15, 30, and 60 min at 37°C. Cells were then washed in heparin (50 U/ml) to release cell surface-associated *DiI*-TRL and bLPL. Fluorescence detection was performed as in Fig. 3. Quantitative analysis of intracellular-associated fluorescence was measured by a CCD-video camera adapted to a fluorescence image analysis system as described in Materials and Methods. Intensity of fluorescence per surface area (μm^2) is represented by mean ± SD from two consecutive and representative experiments. The area analyzed for each condition was about 7,200 μm^2.

The precise localization of the bLPL-binding sites was subsequently studied by immunocytochemistry in cryoultrasections using electron microscopy. After binding at 4°C, most of the bLPL was found along the plasma membrane of microvilli (**Fig. 2A**). Very few of the gold particles were associated with the plasma membrane base of the microvilli or other plasma membrane structures, such as coated pits or caveolae. This indicated that the binding sites for LPL were almost exclusively located on microvilli membranes. To test whether the bound bLPL was internalized, cells were incubated for different periods at 37°C. The bLPL internalization was rather slow. After 30 min incubation, only 20% of the bound bLPL was intracellular and appeared inside non-coated endocytic vesicles (Fig. 2B). The remaining gold particles were still associated with the microvillar membrane. After 1 h at 37°C, about 40–50% of the total immunolabeled bLPL remained bound to the microvilli. Internalized bLPL was found in intracellular vesicles and in multivesicular bodies, which probably correspond to the late endosomes (Figs. 2C and 2D).

bLPL-mediated binding and uptake of *DiI*-TRL by HepG2 cells

The distribution pattern of bound TRL on the surface of cultured HepG2 was studied by binding experiments in the absence or presence of bLPL. Because HepG2 cell synthesize apoE, detection of internalized lipoproteins could not be performed by using antibodies against this apoprotein. Lipoproteins were detected by direct-fluorescence (*DiI*-labeled) and bLPL was detected by immunofluorescence. **Figure 3** shows the binding of *DiI*-TRL in the absence or the presence of bLPL. Bound lipoproteins without bLPL were distributed as small fluorescent spots on the apical surface of HepG2 cells (as detected in vertical sections). The fluorescence was not associated with microvilli. In the pres-

Fig. 5. Uptake of *DiI*-TRL by HepG2 cells in the presence of bLPL. HepG2 cells were incubated for 45 min at 4°C with *DiI*-TRL in the presence bLPL, and incubated for 3, 15, 30, and 60 min at 37°C. Cells were washed in heparin (50 U/ml) to release cell surface-associated *DiI*-TRL and bLPL. Fluorescence detection was performed as in Fig. 3. A three-dimensional projection of six horizontal sections (*xy*, 0.31 µm; step size 0.64 µm) and vertical sections (*xz*, 0.82 µm) was viewed by a confocal microscope. Images correspond to the fluorescence of the ligand underlined. *DiI*-TRL (TRL) internalized progressively in the presence of bLPL during the different times for the uptake experiment (*xy* projections). Some *DiI*-TRL and bLPL (bLPL) colocalized during the first minutes of internalization (*xy* projections; short arrows) as also observed in *xz* sections (fine arrows). At 60 min, the fluorescence of *DiI*-TRL was more intense than that of bLPL (*xy* and *xz* sections). Loss of colocalization between *DiI*-TRL and bLPL was detected at 15 min and it became more evident after 1 h (large arrows). Bar for *xy* projections and for *xz* sections: 25 µm. up: upper part of the cell; lo: lower part of the cell.

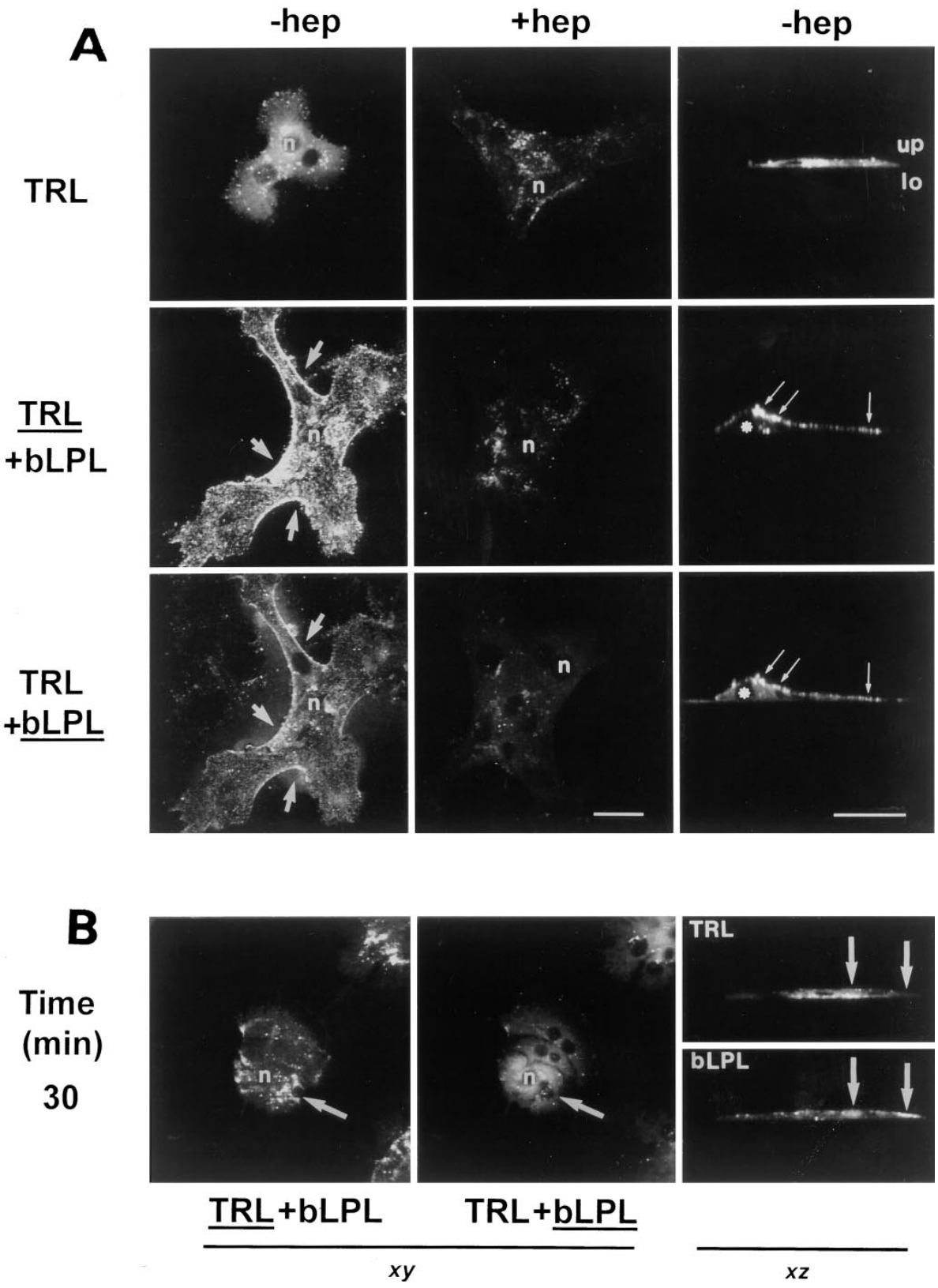

Figure 7.

ence of bLPL, increased intensity of cell surface-associated fluorescence was observed. *DiI* fluorescence completely colocalized with bLPL (Fig. 3), and displayed the same characteristic binding pattern at the microvillar surface as that found when cells were incubated with bLPL alone (Fig. 1). In vertical sections observed with the confocal microscope, the colocalization between bLPL and *DiI*-TRL was also complete and restricted to the upper surface of HepG2 cells. This result was observed whether the molecules were added together or sequentially. Identical patterns were observed when unlabeled TRL was used and detection with anti-apoE (results not shown), indicating that labeling with *DiI* did not influence the binding properties of the lipoprotein particle and also indicating that *DiI* is a suitable marker for the lipoprotein particles. The presence of heparin (50 U/ml) reduced the cell surface-associated fluorescence to background levels and efficiently displaced bound *DiI*-TRL and bLPL (Figs. 3 and 4), indicating that binding sites are sensitive to heparin. Relative quantification of the fluorescence associated with the cell surface (**Fig. 4**) indicated that the presence of bLPL induced a significant increase in the binding of *DiI*-TRL. The amount of bLPL bound to the cell surface did not change as a consequence of the presence of TRL, indicating that lipoproteins did not influence the cell surface-association of bLPL.

Next, experiments on *DiI*-TRL uptake were performed. Binding experiments were performed at 4°C as above and then cells were incubated at 37°C for up to 1 h. At the end of each incubation time, cells were briefly washed in heparin (50 U/ml) to release cell surface-associated (non-internalized) lipoproteins and bLPL. Confocal microscopy analysis of *DiI*-TRL incubated in the presence of bLPL (**Fig. 5**) showed colocalization of the internalized ligands at short times of incubation. However, a progressive loss of colocalization began to appear at 15 min of incubation and became extensive after 1 h at 37°C. At this time the intensity of labeling of bLPL was lower than that of *DiI*-TRL and a high number of *DiI* spots did not colocalize with bLPL immunofluorescence (Fig. 5). Quantification of the internalized fluorescence (**Fig. 6**) after 3 min at 37°C showed that very little *DiI*-TRL or bLPL was internalized by HepG2 cells when incubated together. At this time the amount of *DiI*-TRL internalized in the absence of bLPL was double that internalized in its presence. At longer times at 37°C, internalization of *DiI*-TRL increased, but a plateau was reached between 30 and 60 min of incubation. In contrast, in the presence of bLPL, *DiI*-TRL was internalized progressively for up to 1 h and a plateau was not reached. At this time, more *DiI*-TRL had entered the cells when incubated in the presence of bLPL. Uptake of bLPL in the presence of *DiI*-TRL was also slightly higher than in its absence, but the difference with bLPL incubated alone was not statistically significant.

bLPL-mediated binding and uptake of *DiI*-TRL by hepatocytes

To determine whether hepatocytes in primary culture could also bind and internalize *DiI*-TRL and bLPL, we used rat hepatocytes obtained by collagenase perfusion. As shown in **Fig. 7A** and **Fig. 8A**, hepatocytes bound *DiI*-TRL and bLPL with a pattern similar to HepG2 cells. High magnification evaluation of the confocal fluorescence images showed that both bLPL and *DiI*-TRL in the presence of bLPL bound to the hepatocyte microvilli (not shown). Confocal microscopy analysis of *diI*-TRL and bLPL showed that in the absence of bLPL, *DiI*-TRL that bound to the hepatocyte surface appeared as small fluorescent spots, mostly located in the perinuclear region. However, bLPL-binding sites covered the whole apical surface of hepatocytes (Fig. 7A). When *DiI*-TRL was incubated with bLPL, the fluorescence shown by *DiI*-TRL had the same pattern as bLPL immunofluorescence. A strong colocalization signal of *DiI*-TRL and bLPL was also evident at the upper surface of the hepatocytes in confocal vertical sections (Fig. 7A). This indicates that bLPL mediates the binding of *DiI*-TRL at the surface of hepatocytes. When ligands were incubated in the presence of heparin (50 U/ml) cell surface-associated fluorescence was re-

Fig. 7. Binding and internalization of *DiI*-TRL by cultured hepatocytes in the presence or absence of bLPL. Hepatocytes were treated as described in Fig. 3 and Fig. 5. For binding experiments (A), *DiI*-TRL were incubated for 45 min at 4°C with or without bLPL, and in the presence (+hep) or absence (−hep) of heparin (50 U/ml). For uptake experiments (B), hepatocytes were incubated for 30 min at 37°C and cell surface-associated *DiI*-TRL and bLPL were released with heparin (50 U/ml). After washing and fixation, bLPL was detected with monoclonal 5D2 antibody followed by *FITC*-conjugated rabbit anti-mouse immunoglobulins. A three-dimensional projection of six horizontal sections (*xy*, 0.31 μm; step size 0.72 μm) and vertical sections (*xz*, 0.79 μm) was viewed on a confocal microscope. Images correspond to the fluorescence of the ligand underlined. In the absence of bLPL weak perinuclear binding of *DiI*-TRL (TRL) was observed on the apical surface (up). Colocalization between *DiI*-TRL (TRL + bLPL) and bLPL (TRL + bLPL) is indicated by short arrows in *xy* projections and by fine arrows in *xz* sections. Heparin abolished most of the cell surface-associated fluorescence for both *DiI*-TRL (TRL and TRL + bLPL) and bLPL (TRL + bLPL). In uptake experiments (30 min, 37°C), both bLPL and *DiI*-TRL were detected inside hepatocytes. However, there was no colocalization between the ligands (large arrows in *xy* projection and in *xz* sections). Bar for *xy* projections and for *xz* sections: 25 μm. n and asterisk: nucleus; up: upper side of the cells; lo: lower side of the cells.

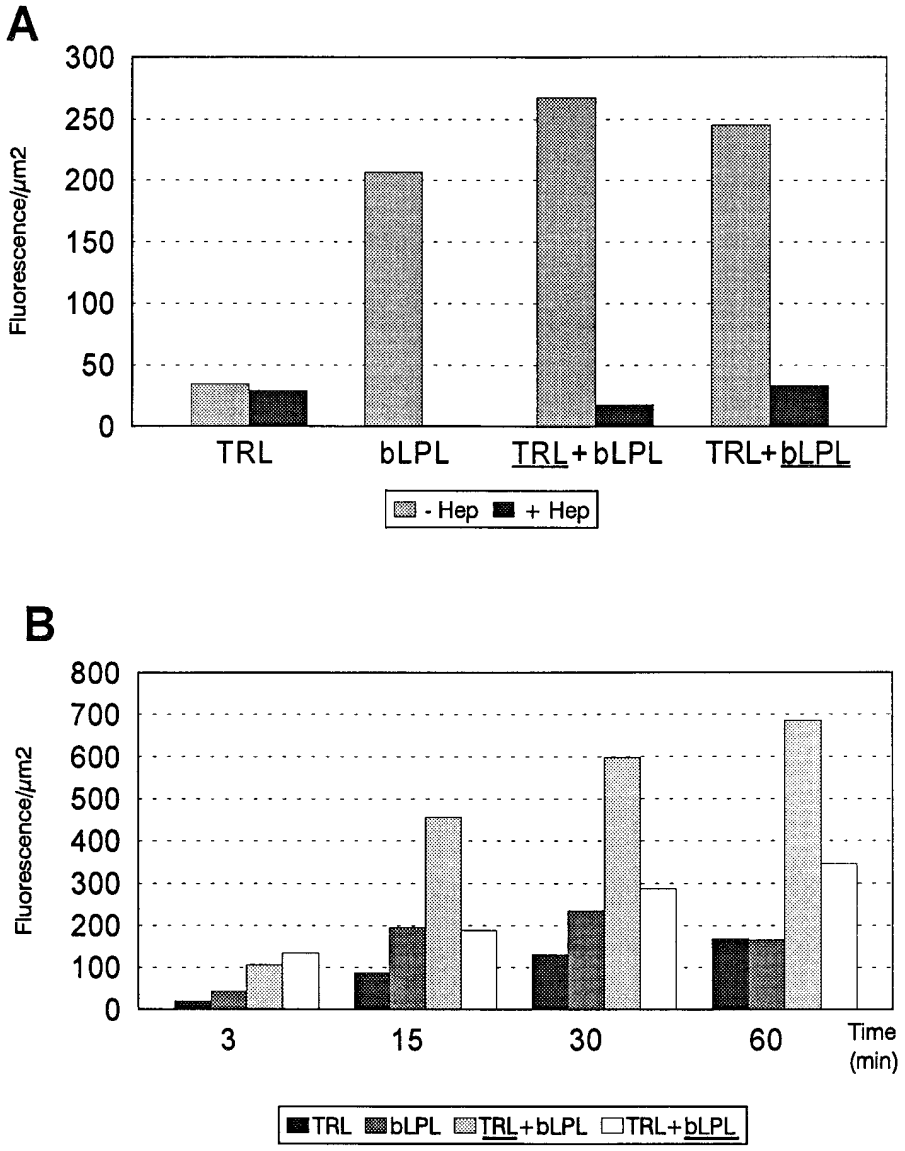

Fig. 8. Quantification of cell surface-associated and internalized fluorescence for bLPL and *DiI*-TRL in the presence or absence of bLPL. (A) Binding experiments. (B) Uptake experiments. Experimental conditions for binding experiments were as in Fig. 7. For internalization, hepatocytes were incubated for 45 min at 4°C with bLPL and *DiI*-TRL in the presence or absence of bLPL, and then incubated for 3, 15, 30, and 60 min at 37°C. Cells were washed in heparin (50 U/ml) to release cell surface-associated *DiI*-TRL and bLPL. Surface and intracellular fluorescence was measured by a CCD-video camera connected to a fluorescence image analysis system as described in Materials and Methods. Intensity of fluorescence per surface area (μm^2) is represented by the mean of eight measures for each experimental condition from one representative experiment. The variation between the different measures did not exceed ± 10% of the mean. The area analyzed for each condition was about 8,200 μm^2.

duced to background levels (Fig. 7A). As in HepG2 cells, confocal analysis of internalized *DiI*-TRL and bLPL at 37°C (Fig. 7B) showed that the colocalization of the two ligands disappeared at 30 min incubation. In binding experiments, cell surface-associated *DiI*-TRL fluorescence was about 10 times higher in the presence of bLPL than in its absence. As in HepG2 cells the presence of *DiI*-TRL did not influence the bLPL binding at the hepatocyte surface, and heparin abolished binding of bLPL and *DiI*-TRL when incubated in the presence of bLPL (Fig. 8A). bLPL-mediated binding of *DiI*-TRL was higher in hepatocytes than in HepG2 cells. Ligand uptake by hepatocytes was quantified as above for up to 1 h at 37°C (Fig. 8B). As observed in HepG2 cells in the absence of bLPL, a plateau of internalized *DiI*-TRL was reached at 30 min of incubation. In contrast, when *DiI*-

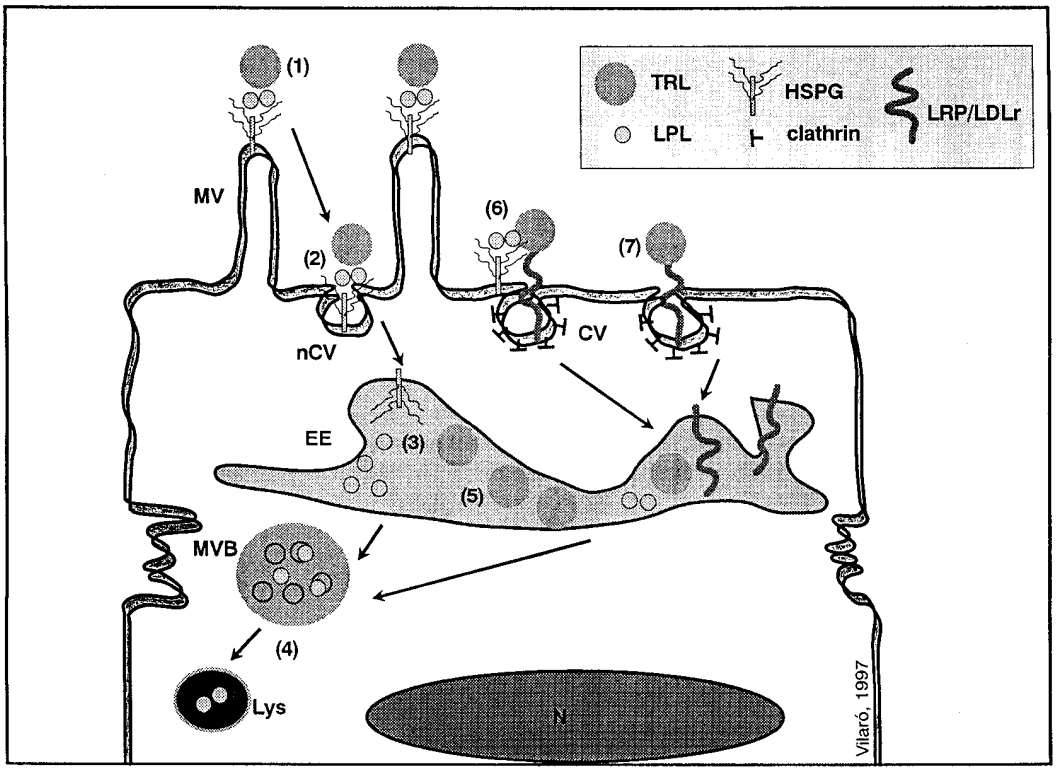

Fig. 9. A postulated model for LPL-mediated binding and uptake of TRL by HepG2 cells and cultured hepatocytes. This model is based on published results and those obtained in the present study. 1) Primary binding-sites for LPL and LPL-TRL are heparan sulfate proteoglycans (HSPG), which are distributed mostly on the microvilli (MV); 2) LPL together with associated TRL are internalized by HSPG in non-coated pit vesicles (nCV); 3) after uptake, these vesicles meet or fuse to early endosomes (EE), where LPL and TRL could separate; 4) LPL is delivered to multivesicular bodies (MVB) and probably to lysosomes (Lys); 5) TRL are retained either within the same early endosomes or in other compartments; 6) alternatively, some LPL and LPL-associated TRL bound to HSPG could be recognized and taken up by LRP or by LDLr following the coated pit (cv) endocytosis pathway to the lysosomes; 7) in the absence of LPL, TRL are recognized and internalized by coated pit-associated receptors. N, nucleus.

TRL was incubated in the presence of bLPL, a progressive increase in internalized fluorescence was observed up to 60 min of incubation at 37°C. After 1 h at 37°C internalized bLPL was higher in the presence of *DiI*-TRL than in its absence, suggesting that the presence of lipoproteins also facilitates internalization of bLPL.

DISCUSSION

LPL potentiates the binding and uptake of chylomicrons, VLDL, and LDL by different cell types, including hepatoma cells, fibroblasts, monocytes, and macrophages and by the perfused liver. The current model states that the increased binding and uptake of LDL and VLDL is due to the bridging of LPL between the lipoproteins and the HSPG that are present on the plasma membrane. Alternatively, both LPL and LPL-associated TRL could be internalized by LRP (26). In the present study we show that: *i*) binding of bLPL occurs at the microvillar surface of HepG2 cells and that bLPL is internalized following a slow endocytic process; *ii*) the cell surface distribution and internalization of TRL by HepG2 and cultured hepatocytes differs depending on the presence of bLPL, and *iii*) after internalization, bLPL and TRL follow different intracellular routes. All these results provide new evidence for the LPL-mediated uptake of TRL and suggest that the mechanisms for binding and uptake of TRL in liver could be dissimilar, depending on the presence of LPL.

Binding of LPL on the surface of liver cells

Binding of bLPL occurs at the microvillar surface of HepG2 cells and hepatocytes. These bindings sites appear different from those previously found on fibroblasts (40–42). This difference may be due to the fact that HepG2 cells and hepatocytes are typical epithelial cells while fibroblasts are mesenchymal cells, which have few, short microvilli on their surface. Moreover,

both the intracellular and the cell surface molecular organization of these cells types are very different (46). In the capillary endothelium of heart, LPL was also found at the surface of microvilli-like luminal surface projections (47). The distribution of bLPL on the microvilli of HepG2 and hepatocytes coincides with that observed for HSPG, which concentrate on the membrane microvilli in the space of Disse of the hepatocyte (48, 49). In addition, binding of bLPL to the surface of HepG2 cells is markedly reduced by heparin or heparinase treatment (11, 16, 17, 21, 24, 30). Together with our present results this indicates that HSPG could be the microvillar-binding sites for bLPL. In liver, the hepatocyte microvilli are the main components of the space of Disse. Thus, if LPL-binding sites concentrate in this plasma domain they are more likely to interact with circulating LPL. All this supports the hypothesis proposed by several authors (13, 14, 16, 17, 21, 24) that HSPG are the main cell receptors for LPL, although the possibility that some LPL could also bind to other cell surface receptors, like LRP (9), cannot be ruled out.

LPL-mediated binding of TRL

DiI labels the surface of the TRL and therefore could influence the binding of lipoprotein particles and some could dissociate during lipolysis by LPL. Previous studies have used *DiI* to follow the intracellular fate of TRL (50). In the present study identical patterns of cell surface distribution were observed for *DiI*-TRL and unlabeled TRL detected with anti-apoE and immunofluorescence, suggesting that *DiI* did not influence the cell binding properties of the lipoprotein particle. In a recent study (41) we performed a morphological study in fibroblasts of the intracellular fate of *DiI*-TRL visualized by fluorescence and TRL by immunofluorescence and immunogold electron microscopy using anti-apoE. The data indicated that for up to 1 h of incubation the intracellular distribution of *DiI* and apoE fluorescence remains in the lipid particle after binding and uptake. However, as it is not possible to estimate the proportion of the *DiI* label that is released back from the TRL particle after 37°C incubation in the presence of bLPL, the data obtained could be an underestimation of the total *DiI* fluorescence taken up by the cells.

The presence of bLPL caused a marked increase in the cell-surface binding of *DiI*-TRL, and quantitative fluorescence indicates that *DiI*-TRL did not influence binding of bLPL at the cell surface. When TRL were incubated with bLPL at 4°C, the distribution of bound bLPL and TRL was totally coincident and covered all the apical surface of HepG2 cells and hepatocytes. Previous ultrastructural studies in fibroblasts showed that immunofluorescence colocalization between bLPL and TRL implies close association between bLPL and the lipoprotein particle (41). Thus, the present results suggest that bLPL acts as a bridge between HSPG and TRL on the microvillar surface of HepG2 cells and hepatocytes. However, in the absence of bLPL, binding of TRL was lower and concentrated in a perinuclear region, suggesting that TRL bound to cell surface receptors other than HSPG. It is now well established that coated-pit receptors (such as LDLr and LRP) are mostly concentrated in perinuclear regions (41) and these structures comprise only 2% of the total cell surface (51). Thus, it is likely that in the absence of LPL, most of the TRL bind to lipoprotein receptors located in coated-pits, which in turn are responsible for their further endocytosis.

LPL-mediated uptake of TRL

After binding to the apical microvilli, bLPL was internalized by HepG2. As internalized bLPL was detected in membrane vesicles and in late endosomes and multivesicular bodies, the present study demonstrated that bLPL uptake follows an endocytic pathway. However, endocytosis of bLPL was slower than other ligands that bind to coated-pit-associated receptors, which have a half-life at the plasma membrane of about 10–20 min (51). Endocytosis of HSPG is usually slow with a half-life of about 4 h (52–54). Here we found that in HepG2, which behaves in a way similar to fibroblasts (41) at longer times of incubation, a large proportion of the bLPL (about 50% at 1 h) remained at the cell surface, suggesting that the HSPG that bind bLPL to the microvilli could also be responsible for internalization.

Further support for the hypothesis that internalization of the LPL did not follow the classical pathway comes from the quantitative fluorescence. The time-course of the internalization of fluorescence associated with *DiI*-TRL and bLPL was different: *DiI*-TRL was quickly internalized by both HepG2 cells and hepatocytes and reached a plateau at 30 min, whereas intracellular bLPL increased continuously during the incubation. Taken together, these results suggest that the ligands, when incubated separately, followed different internalization routes that could be dependent on the cell surface receptor that recognizes the ligands. TRL in the absence of LPL could be recognized by coated-pit-associated receptors of hepatocytes, such as LRP or LDLr (26, 55). However, when *DiI*-TRL was incubated in the presence of bLPL, they presented the same intracellular fluorescence kinetics as bLPL. This indicates that LPL, in addition to bridging TRL to the HSPG, also drives and stimulates the uptake of TRL in a non-saturatable manner. As the abundance of plasma membrane HSPG is higher than the number of high-affinity receptors for lipoproteins, the physiological relevance

of these results could be that when LPL is present, internalization of lipoproteins is slower, but it follows a non-down-regulated endocytosis pathway. However, in the absence of LPL, the rate-limiting mechanism of TRL internalization may be the number of plasma membrane receptors available for the ligands.

Provided that a portion of the *DiI* remained associated with the internalized TRL particle when incubated in the presence of bLPL, the loss of codistribution between bLPL and TRL at short times (15 min) suggests that after uptake, the coligands followed different pathways. This was also suggested by the increase in the intracellular fluorescence of *DiI*-TRL when incubated in the presence of bLPL, which was about 22-fold in hepatocytes from 3 min to 1 h of incubation. In contrast, the increase of bLPL immunofluorescence was only one-tenth of this in the same incubation period. Previous studies by Lombardi et al. (18, 56) showed that LPL-treated VLDL and VLDL are slowly degraded by HepG2 cells. In addition, the same authors showed that LPL-treated VLDL and VLDL undergo retro-endocytosis, possibly as a consequence of a long residence time in early endosomes. Our present fluorescence studies are consistent with this conclusion and suggest that internalized LPL separates from TRL at an early stage of endocytosis and could be directed to lysosomes for degradation (21). This may explain the loss of colocalization between LPL and *DiI*-TRL and why the fluorescence of bLPL did not increase at the same rate as *DiI*-TRL.

In summary, the results obtained in the present study, together with those already published, allow us to postulate the following model for LPL-mediated binding and uptake of TRL by HepG2 and hepatocytes (**Fig. 9**). *1*) Binding of LPL associated with the surface of TRL occurs at the HSPG of the microvilli; *2*) after binding, LPL and TRL are internalized by the HSPG in non-coated pit vesicles; *3*) these vesicles meet or fuse to early endosomes, where it is likely that LPL and TRL separate; *4*) LPL is delivered to multivesicular bodies and probably to the lysosomes, where it is degraded; *5*) TRL is retained either within the same early endosomes or in other compartments; *6*) alternatively (or in parallel), some LPL and LPL-associated TRL could be bound and taken up by LRP following the classical endocytosis pathway to the lysosomes; *7*) in the absence of LPL, TRL are recognized and internalized by coated pit-associated receptors.

Remnant lipoproteins are cleared rapidly from the circulation by the liver, where they accumulate in the space of Disse. Retention of remnant lipoproteins is essential for the acquisition of hepatocyte-secreted apoE (3). ApoE is also a heparin-binding protein (57–60). Hepatocyte-secreted apoE accumulates in the space of Disse and is found associated with the microvilli and endocytic structures (61). The apoE-enriched particles are thus retained through the apoE-mediated binding to membrane HSPG. Furthermore, it has been shown that apoE increases the uptake of lipoproteins by hepatocyte receptors like the LDL-receptor (3, 55, 57, 62) and the LPR (55, 63–67) via receptor-mediated endocytosis. Studies on LPL metabolism indicate that the enzyme is released from the endothelial surfaces of extrahepatic tissues to the blood (2) and is subsequently taken up and degraded by the liver (7, 8). In plasma, LPL circulates in association with lipoproteins (5, 6). LPL associated with circulating lipoproteins may mediate the first retention of these lipoproteins in the space of Disse through its binding to HSPG at the membrane microvilli, thus facilitating the subsequent acquisition of hepatocyte-secreted apoE by the lipoproteins. In turn, apoE may also be involved in the further retention of lipoproteins by HSPG, inhibiting hydrolysis by LPL (66) and stimulating binding of LPL to HSPG (67). Both LPL and apoE eventually facilitate the uptake of lipoproteins through their binding to cell HSPGs, either by internalization of HSPG themselves (slow pathway) or by the presentation of the lipoproteins to specific lipoprotein receptors responsible for receptor-mediated endocytosis (fast pathway).

We thank Susanna Castel (Serveis Cientifico-Tecnics de la Universitat de Barcelona) for her constant help and expert assistance with the confocal microscope, and David García for his expert technical assistance with cell lines. We are grateful to David Bellido and Roser Buscà for their help in the cryoultramicrotomy experiments in Figure 2 and to Mar Fernández, who performed some experiments at the beginning of this work. We are very grateful to Dr. Ulrike Beisiegel for useful comments and discussions. We also thank Robin Rycroft for his expert editorial help. This work was supported by the Comisión Interministerial de Ciencia y Tecnología (grant PB94-1548), the Fondo de Investigaciones Sanitarias from Ministerio de Sanidad (grant 96/2099), and BIOMED program of the European Community (grant PL-921243).

Manuscript received 9 June 1997, in revised form 3 November 1997, and in re-revised form 24 December 1997.

REFERENCES

1. Olivecrona, G., and T. Olivecrona. 1995. Triglyceride lipases atherosclerosis. *Curr. Opin. Lipidol.* **6:** 291–305.
2. Goldberg, I. J. 1996. Lipoprotein lipase and lipolysis: central roles in lipoprotein metabolism and atherogenesis. *J. Lipid Res.* **37:** 693–707.
3. Mahley, R. W., and M. M. Hussain. 1991. Chylomicron and chylomicron remnant catabolism. *Curr. Opin. Lipidol.* **2:** 170–176.

4. Felts, J. M., H. Itakura, and R. T. Crane. 1975. The mechanism of assimilation of constituents of chylomicrons, very low density lipoproteins and remnants—a new theory. *Biochem. Biophys. Res. Commun*. **66:** 1467–1475.
5. Goldberg, I. J., J. J. Kandel, G. B. Blum, and H. N. Ginsberg. 1986. Association of plasma lipoproteins with post-heparin lipase activities. *J. Clin. Invest*. **78:** 1523–1528.
6. Vilella, E., J. Joven, M. Fernández, S. Vilaró, J. D. Brunzell, T. Olivecrona, and G. Bengtsson-Olivecrona. 1993. Lipoprotein lipase in human plasma is mainly inactive and associated with cholesterol-rich lipoproteins. *J. Lipid Res.* **34:** 1555–1564.
7. Wallinder, L., J. Peterson, T. Olivecrona, and G. Bengtsson-Olivecrona. 1984. Hepatic and extrahepatic uptake of intravenously injected lipoprotein lipase. *Biochim. Biophys. Acta*. **795:** 513–524.
8. Vilaró, S., M. Llobera, G. Bengtsson-Olivecrona, and T. Olivecrona. 1988. Lipoprotein lipase uptake from the liver: localization, turnover, and metabolic role. *Am. J. Physiol*. **254:** G711–G722.
9. Beisiegel, U., W. Weber, and G. Bengtsson-Olivecrona. 1991. Lipoprotein lipase enhances the binding of chylomicrons to low density lipoprotein receptor-related protein. *Proc. Natl. Acad. Sci. USA*. **88:** 8342–8346.
10. Mulder, M., E. de Wit, and L. M. Havekes. 1991. The binding of human lipoprotein lipase treated VLDL by the human hepatoma cell line HepG2. *Biochim. Biophys. Acta*. **1081:** 308–314.
11. Eisenberg, S., E. Sehayek, T. Olivecrona, and I. Vlodavsky. 1992. Lipoprotein lipase enhances binding of lipoproteins to heparan sulfate on cell surfaces and extracellular matrix. *J. Clin. Invest.* **90:** 2013–2021.
12. Williams, K. J., K. A. Petrie, R. W. Brocia, and T. L. Swenson. 1991. Lipoprotein lipase modulates net secretory output of apolipoprotein B in vitro. *J. Clin. Invest.* **88:** 1300–1306.
13. Williams, K. J., G. M. Fless, K. A. Petrie, M. L. Snyder, R. W. Brocia, and T. L. Swenson. 1992. Mechanisms by which lipoprotein lipase alters cellular metabolism of lipoprotein, low density lipoprotein, and nascent lipoproteins. *J. Biol. Chem.* **267:** 13284–13292.
14. Rumsey, S. C., J. C. Obunike, Y. Arad, R. J. Deckelbaum, and I. J. Goldberg. 1992. Lipoprotein lipase-mediated uptake and degradation of low density lipoproteins by fibroblasts and macrophages. *J. Clin. Invest.* **90:** 1504–1512.
15. Evans, A. J., C. G. Sawyez, B. M. Wolfe, and M. W. Huff. 1992. Lipolysis is a prerequisite for lipid accumulation in HepG2 cells induced by large hypertriglyceridemic very low density lipoproteins. *J. Biol. Chem.* **267:** 10743–10751.
16. Mulder, M., P. Lombardi, H. Jansen, T. J. C. van Berkel, R. R. Frants, and L. M. Havekes. 1992. Heparan sulphate proteoglycans are involved in the lipoprotein lipase-mediated enhancement of the cellular binding of very low density and low density lipoproteins. *Biochem. Biophys. Res. Commun*. **185:** 582–587.
17. Mulder, M., P. Lombardi, H. Jansen, T. J. C. van Berkel, R. R. Frants, and L. M. Havekes. 1993. Low density lipoprotein receptor internalizes low density and very low density lipoproteins that are bound to heparan sulfate proteoglycans via lipoprotein lipase. *J. Biol. Chem.* **268:** 9369–9375.
18. Lombardi, P., M. Mulder, E. de Wit, T. J. C. van Berkel, R. R. Frants, and L. M. Havekes. 1993. Low-density lipoproteins are degraded in HepG2 cells with low efficiency. *Biochem. J.* **290:** 509–514.
19. Obunike, J. C., I. J. Edwards, S. C. Rumsey, L. K. Curtiss, W. D. Wagner, R. J. Deckelbaum, and I. J. Goldberg. 1994. Cellular differences in lipoprotein lipase-mediated uptake of low density lipoproteins. *J. Biol. Chem.* **269:** 13129–13135.
20. Krapp, A., H. Zhang, D. Ginzinger, M-S. Liu, A. Lindberg, G. Olivecrona, M. R. Hayden, and U. Beisiegel. 1995. Structural features in lipoprotein lipase necessary for the mediation of lipoprotein uptake into cells. *J. Lipid Res.* **36:** 2362–2373.
21. Sehayek, E., T. Olivecrona, G. Bengtsson-Olivecrona, I. Vlodavsky, H. Levkovitz, R. Avner, and S. Eisenberg. 1995. Binding to heparan sulfate is a major event during catabolism of lipoprotein lipase by HepG2 and other cell cultures. *Atherosclerosis.* **114:** 1–8.
22. Chang, S., N. Maeda, and J. Borensztajn. 1996. The role of lipoprotein lipase and apoprotein E in the recognition of chylomicrons and chylomicron remnants by cultured isolated mouse hepatocytes. *Biochem. J.* **318:** 29–34.
23. Cianflone, K., R. K. Avramoglu, C. Sawyez, and M. W. Huff. 1996. Inhibition of lipoprotein lipase-induced cholesteryl ester accumulation in human hepatoma HepG2 cells. *Atherosclerosis.* **120:** 101–114.
24. Fuki, I. V., K. M. Kuhn, I. R. Lomazov, V. L. Rothman, G. P. Tuszynski, R. V. Iozzo, T. L. Swenson, E. A. Fisher, and K. J. Williams. 1997. The syndecan family of proteoglycans. Novel receptors mediating internalization of atherogenic lipoproteins in vitro. *J. Clin. Invest.* **100:** 1611–1622.
25. Skottova, N., R. Savonen, A. Lookene, M. Hultin, and G. Olivecrona. 1995. Lipoprotein lipase enhances removal of chylomicrons and chylomicron remnants by the perfused rat liver. *J. Lipid Res.* **36:** 1334–1344.
26. Beisiegel, U. 1995. Receptors for triglyceride-rich lipoproteins and their role in lipoprotein metabolism. *Curr. Opin. Lipidol.* **6:** 117–122.
27. Beisiegel, U. 1996. New aspects on the role of plasma lipases in lipoprotein catabolism and atherosclerosis. *Atherosclerosis.* **124:** 1–8.
28. Olivecrona, T., and G. Bengtsson-Olivecrona. 1989. Heparin and lipases. *In* Heparin. C. D. Lane, and U. Lindahl, editors. Edward Arnold, London. 335–361.
29. Lookene, A., O. Chevreuil, P. Ostergaard, and G. Olivecrona. 1996. Interaction of lipoprotein lipase with heparan sulfate: stoichiometry, stabilization, and kinetics. *Biochemistry.* **35:** 12155–12163.
30. Chapell, D. A., G. L. Fry, M. A. Waknitz, L. E. Muhonen, M. W. Pladet, P-H. Iverius, and D. K. Strickland. 1993. Lipoprotein lipase induces catabolism of normal triglyceride-rich lipoproteins via the low density lipoprotein receptor-related protein/α_2-macroglobulin receptor in vivo. *J. Biol.Chem.* **268:** 14168–14175.
31. Nykjaer, A., G. Bengtsson-Olivecrona, A. Lookene, S. K. Moestrup, C. M. Petersen, W. Weber, U. Beisiegel, and J. Gliemann. 1993. The α_2-macroglobulin receptor/low density lipoprotein receptor related protein binds lipoprotein lipase and β-migrating very low density lipoprotein associated with the lipase. *J. Biol. Chem.* **268:** 15048–15055.
32. Nielsen, M. S., A. Nykjaer, I. Warshawsky, A. L. Schwartz, and J. Gliemann. 1995. Analysis of ligand binding to the alpha 2-macroglobulin receptor/low density lipoprotein receptor-related protein. Evidence that lipoprotein lipase and the carboxyl-terminal domain of the receptor-associ-

ated protein bind to the same site. *J. Biol. Chem.* **270:** 23713–23719.
33. Nielsen, M. S., J. Brejning, R. García, H. Zhang, M. R. Hayden, S. Vilaró, and J. Gliemann. 1997. Segments in the c-terminal folding domain of lipoprotein lipase important for binding to the low density lipoprotein receptor-related protein and to heparan sulfate proteoglycans. *J. Biol. Chem.* **272:** 5821–5827.
34. Chappell, D. A., I. Inoue, G. L. Fry, M. W. Pladet, S. L. Bowen, P-H. Iverius. J-M. Lalouel, and D. K. Strickland. 1994. Cellular catabolism of normal very low density lipoproteins via the low density lipoprotein receptor-related protein / α_2-macroglobulin receptor is induced by the c-terminal domain of lipoprotein lipase. *J. Biol. Chem.* **269:** 18001–18006.
35. Medh, J. D., S. L. Bowen, G. L. Fry, S. Rubén, M. Andrakl, I. Inoue, J. M. Lalouel, D. K. Strickland, and D. A. Chappell. 1996. Lipoprotein lipase binds to low density lipoprotein receptors and induces receptor-mediated catabolism of very low density lipoproteins in vitro. *J. Biol. Chem.* **271:** 17073–17080.
36. Argraves, K. M., F. D. Battey, C. D. MacCalman, K. R. McCrae, M. Gafvels, K. F. Kozarsky, D. A. Chappell, J. F. Strauss III, and D. K. Strickland. 1995. The very low density lipoprotein receptor mediates the cellular catabolism of lipoprotein lipase and urokinase-plasminogen activator inhibitor type I complexes. *J. Biol. Chem.* **270:** 26550–26557.
37. Takahashi, S., J. Suzuki, M. Kohno, K. Oida, T. Tamai, S. Miyabo, T. Yamamoto, and T. Nakai. 1995. Enhancement of the binding of triglyceride-rich lipoprotein to the very low density lipoprotein receptor by apolipoprotein E and lipoprotein lipase. *J. Biol. Chem.* **270:** 15747–15754.
38. Willnow, T. E., J. L. Goldstein, K. Orth, M. S. Brown, and J. Herz. 1992. Low density lipoprotein receptor-related protein and gp330 bind similar ligands, including plasminogen activator–inhibitor complexes and lactoferrin, an inhibitor of chylomicron remnant clearance. *J. Biol. Chem.* **267:** 26172–26180.
39. Kounnas, M. Z., D. A. Chappell, D. K. Strickland, and W. S. Argraves. 1993. Glycoprotein 330, a member of the low density lipoprotein receptor family, binds lipoprotein lipase in vitro. *J. Biol. Chem.* **268:** 14176–14181.
40. Fernández-Borja, M., D. Bellido, R. Makiya, G. David, G. Olivecrona, M. Reina, and S. Vilaró. 1995. The actin cytoskeleton of fibroblasts organizes surface proteoglycans that bind basic fibroblasts growth factor and lipoprotein lipase. *Cell Motil. Cytoskel.* **30:** 89–107.
41. Fernández-Borja, M., D. Bellido, E. Vilella, G. Olivecrona, and S. Vilaró. 1996. Lipoprotein lipase-mediated uptake of lipoprotein in human fibroblasts: evidence for an LDL receptor-independent internalization pathway. *J. Lipid Res.* **37:** 464–481.
42. Martinho, R. G., S. Castel, J. Ureña, M. Fernández-Borja, R. Makiya, G. Olivecrona, M. Reina, A. Alonso, and S. Vilaró. 1996. Ligand binding to heparan sulfate proteoglycans induces their aggregation and distribution along actin cytoskeleton. *Mol. Biol. Cell.* **7:** 1771–1788.
43. Bengtsson-Olivecrona, G., and T. Olivecrona. 1991. Phospholipase activity of milk lipoprotein lipase. *Methods Enzymol.* **197:** 345–356.
44. Berry, M. N., and D. H. Friend. 1969. High-yield preparation of isolated rat liver parenchymal cells: a biochemical and fine structural study. *J. Cell. Biol.* **43:** 506–520.
45. Innerarity, T. L., R. E. Pitas, and R. W. Mahley. 1986. Receptor interactions. *Methods Enzymol.* **129:** 542–565.
46. Matter, K., and I. Mellman. 1994. Mechanisms of cell polarity: sorting and transport in epithelial cells. *Curr. Opin. Cell Biol.* **6:** 546–554.
47. Blanchette-Mackie, E. J., H. Masuno, N. K. Dwyer, T. Olivecrona, and R. O. Scow. 1989. Lipoprotein lipase in myocytes and capillary endothelium of heart: immunocytochemical study. *Am. J. Physiol.* **256:** E818–E828.
48. Stow, J. L., L. Kjellen, E. Unger, M. Höök, and M. G. Farquhar. 1985. Heparan sulfate proteoglycans are concentrated on the sinusoidal plasmalemmal domain and in intracellular organelles of hepatocytes. *J. Cell Biol.* **100:** 975–980.
49. Roskams, T., H. Moshage, R. De Vos, D. Guido, P. Yap, and V. Desmet. 1995. Heparan sulfate proteoglycan expression in normal human liver. *Hepatology.* **21:** 950–958.
50. Tabas, I., S. Lim, X. X. Xu, and F. R. Maxfield. 1990. Endocytosed beta-VLDL and LDL are delivered to different intracellular vesicles in mouse peritoneal macrophages. *J. Cell Biol.* **111:** 929–940.
51. Goldstein, J. L., S. K. Basu, and M. S. Brown. 1983. Receptor-mediated endocytosis of low-density lipoprotein in cultured cells. *Methods Enzymol.* **98:** 241–260.
52. Uhlin-Hansen, L., and M. Yanagishita. 1995. Brefeldin A inhibits the endocytosis of plasma-membrane-associated heparan sulphate proteoglycans of cultured rat ovarian granulosa cells. *Biochem. J.* **310:** 271–278.
53. Yanagishita, M. 1992. Glycosylphosphatidylinositol-anchored and core protein-intercalated heparan sulfate proteoglycans in rat ovarian granulosa cells have distinct secretory, endocytic, and intracellular degradative pathways. *J. Biol. Chem.* **267:** 9505–9511.
54. Gleizes, P-E, J. Noaillac-Depeyre, M-A. Dupont, and N. Gas. 1996. Basic fibroblast growth factor (FGF-2) is addressed to caveolae after binding to the plasma membrane of BHK cells. *Eur. J. Cell Biol.* **71:** 144–153.
55. Herz, J., and T. E. Willnow. 1995. Lipoprotein and receptor interaction in vivo. *Curr. Opin. Lipidol.* **6:** 97–103.
56. Lombardi, P., M. Mulder, H. van der Boom, R. R. Frants, and L. M. Havekes. 1993. Inefficient degradation of triglyceride-rich lipoprotein by HepG2 cells is due to a retarded transport to the lysosomal compartment. *J. Biol. Chem.* **268:** 26113–26119.
57. Ji, Z-S., W. J. Brecht, R. D. Miranda, M. M. Hussain, T. L. Innerarity, and R. W. Mahley. 1993. Role of heparan sulfate proteoglycans in the binding and uptake of apolipoprotein E-enriched remnant lipoproteins by cultured cells. *J. Biol. Chem.* **268:** 10160–10167.
58. Ji, Z-S., S. Fazio, Y-L. Lee, and R. W. Mahley. 1994. Secretion-capture role for apolipoprotein E in remnant lipoprotein metabolism involving cell surface heparan sulfate proteoglycans. *J. Biol. Chem.* **269:** 2764–2772.
59. Ji, Z-S., S. Fazio, and R. W. Mahley. 1994. Variable heparan sulfate proteoglycan binding of apolipoprotein E variants may modulate the expression of Type III hyperlipoproteinemia. *J. Biol. Chem.* **269:** 13421–13428.
60. Ji, Z-S., D. A. Sanan, and R. W. Mahley. 1995. Intravenous heparinase inhibits remnant lipoprotein clearance from the plasma and uptake by the liver: in vivo role of heparan sulfate proteoglycans. *J. Lipid Res.* **36:** 583–592.
61. Hamilton, R. L., J. S. Wong, L. S. S. Guo, S. Krisans, and R. J. Havel. 1990. Apolipoprotein E localization in rat

hepatocytes by immunogold labeling of cryothin sections. *J. Lipid Res.* **31:** 1589–1603.
62. Bradley, W. A., and S. H. Gianturco. 1990. Lipoprotein receptors. *Curr. Opin. Lipidol.* **1:** 216–221.
63. Beisiegel U., W. Weber, G. Ihrke, J. Herz, and K. K. Stanley. 1989. The LDL-receptor-related protein, LRP, is an apolipoprotein E-binding protein. *Nature.* **341:** 162–164.
64. Kowal, R. C., J. Herz, J. L. Goldstein, V. Esser, and M. S. Brown. 1989. Low density lipoprotein receptor-related protein mediates uptake of cholesteryl esters derived from apoprotein E-enriched lipoproteins. *Proc. Natl. Acad. Sci. USA.* **86:** 5810–5814.
65. Kowal, R. C., J. Herz, K. H. Weisgraber, R. W. Mahley, M. S. Brown, and J. L. Goldstein. 1990. Opposing effects of apolipoproteins E and C on lipoprotein binding to low density lipoprotein receptor-related protein. *J. Biol. Chem.* **265:** 10771–10779.
66. Rensen, P. C. N., and T. J. C. van Berkel. 1996. Apolipoprotein E effectively inhibits lipoprotein lipase-mediated lipolysis of chylomicron-like triglyceride-rich lipid emulsions in vitro and in vivo. *J. Biol. Chem.* **271:** 14791–14799.
67. van Barlingen, H. H., H. de Jong, D. W. Erkelens, and T. W. Bruin. 1996. Lipoprotein lipase-enhanced binding of human triglyceride-rich lipoproteins to heparan sulfate: modulation by apolipoprotein E and apolipoprotein C. *J. Lipid Res.* **37:** 754–763.